KSCE Journal of Civil Engineering (2014) 18(3):812-818
DOI 10.1007/s12205-014-0384-7
Copyright ©2014 Korean Society of Civil Engineers

Tunnelling and Underground Space Construction for Sustainable Development

pISSN 1226-7988, eISSN 1976-3808
www.springer.com/12205

CFD Analysis on Ventilation Characteristics of Jet Fan with Different Pitch Angle

Seung-Chul Lee*, Seungho Lee, and Juhee Lee*****

Received June 30, 2013/Revised October 1, 2013/Accepted October 24, 2013

Abstract

The objective of this paper is to realize a CFD (Computational Fluid Dynamics) analysis to evaluate the ventilation characteristics of the Banana Jet Fan with different pitch angles (0 ~ 20 degrees) and to determine the optimal angle. The airflow discharged from the jet fan was the highest at $\alpha = 0^{o}$ where the loss from the jet fan itself was the lowest. But the airflow of the tunnel was the highest at $\alpha = 6.0^{o}$. This is due to the significant energy loss from friction at the ceiling of the tunnel when the pitch angle of the jet fan is low ($\alpha = 0^{o}$) and significant energy loss from recirculation, rather than friction loss, when the pitch angle is high ($\alpha = 20^{o}$). Therefore, the highest level of the airflow is at $\alpha = 6.0^{o}$ where the loss from both ceiling and bottom is the least. When designing the jet fan in the tunnel ventilation, these effects of airflow into the tunnel and friction loss must be considered.

Keywords: *banana jet fan, CFD, ventilation, road tunnel*

1. Introduction

Depending on the ventilation type, the road tunnel can be classified largely into the natural ventilation type and the mechanical ventilation type. The natural ventilation type is used when ventilation is required to remove the polluted air and hazardous gas that can interfere with driver's visibility. This can be facilitated by the air flow of the tunnel itself arising from a piston effect of the vehicles driving through the tunnel.

The mechanical ventilation type is applied to long tunnels that cannot be ventilated solely by the natural ventilation of the tunnel itself based on the piston effect of the vehicles driving through the tunnel, and generally this refers to the tunnel which uses a ventilation system to force fresh air outside of the tunnel to flow into the tunnel to dilute the polluted air. This mechanical ventilation type tunnel can be classified into longitudinal flow type tunnel, semi-transverse flow type tunnel and transverse flow type tunnel.

Recently, a number of domestic road tunnels use the longitudinal flow type of mechanical ventilation. The longitudinal flow type tunnel is ventilated by the combination of a jet fan, a vertical shaft, and a dust collector. The advantage of the mechanical ventilation system is as follows: The jet fan is easy to install, is economical due to the reduced equipment cost and can easily respond to the change in traffic. However, it has a disadvantage of creating loud noise from the fan. The vertical shaft type has the advantage of effectively using the ventilation force of the traffic and not having any limitation based on the length of the tunnel, but has the disadvantage of high installation and excavation costs of the underground ventilation chamber or a large-scale fan. Therefore, the vertical shaft type is applied to long large-scale tunnels. The dust collector type can also use the ventilation force of the traffic as the vertical shaft type and is appropriate for tunnels with high foundations and city tunnels, which require external pollution control. But the dust collector type has a disadvantage when responding to fire situations.

The flow structure in the tunnel is critical for the effective ventilation. The flow characteristics of the curved tunnel are different from the normal straight tunnel. Wang *et al.* (2010) carried the computational study to investigate the aerodynamic behavior of jet fans in a curved road tunnel and showed that the variations of the static and dynamic pressure in a curved tunnel were changed non-monotonically. The pressure along the tunnel increases gradually after the jet fan, but this is followed by a sudden drop and then a recovery. A sudden increase in pressure is resulted as the jet passes by the convex wall, whereas that the concave wall is approached causes a pressure reduction. The flow in the curved tunnel becomes asymmetrical downstream.

When the length of the tunnel is long enough, there are a series of jet fans in the tunnel. The ventilation of the polluted air is varied according to the operation of the fans. Se *et al.* (2012) has investigated that the effect of the location of activated fan group on the airflow structure and temperature distribution in a longitudinally ventilated tunnel. The solid fire creates a sudden contraction to the air passageway that should enhance the airflow velocity; however, the upstream velocity is reduced surprisingly.

*Professor, Dept. of Fire Protection Engineering, Kangwon National University, Gangwon-do 245-710, Korea (E-mail: sclee@kangwon.ac.kr)
**Member, Professor, Dept. of Civil Engineering, Sangji University, Gangwon-do 220-702, Korea (E-mail: shsh123@hanmail.net)
***Professor, Dept. of Mechatronics, Hoseo University, Chungcheongnam-do 336-795, Korea (Corresponding Author, E-mail: juheelee@hoseo.edu)

It suggests that the conventional concept of activating the furthest fan group may be sufficient to prevent backlayering for solid fire; instead, the closest fan group or more fans may be needed to provide sufficient airflow velocity.

Domestically, the jet fan type ventilation system is applied mostly to long large-scale tunnels and many domestic researches (Ryu *et al.* 2003; Kweon *et al.* 2006; Byun *et al.* 2007) are in progress.

Recently, a new tunnel ventilation design, the so-called Banana Jet Fan (Witt and Schutze, 2006), has an ability to change the angle of the jet fan inlet/outlet in the jet fan type ventilation system and has been recently introduced. Though the Banana Jet Fan has the advantage of maximizing the ventilation efficiency by reducing the friction loss on the tunnel ceiling of the existing jet fan, but the lack of detailed research still poses challenges in designing the ventilation system of the tunnel.

Therefore, this research analyzes the ventilation characteristics of the Banana Jet Fan installed on a domestic highway based on the jet fan inlet/outlet angle using the CFD method to compare and analyze the ventilation dynamics of each case. Although extensive studies on the ventilation in straight road tunnels have been conducted as seen from the literature review, the authors are unaware of detailed study in a variable pitch angles of a jet fan. The purpose of this study is to investigate the aerodynamic behaviors of jet fans and find the optimal pitch angle that maximizes the air-entrainment and minimizes the energy loss at the same time. The inlet/outlet angle of the jet fan varies from 0 to 20 degree and the comparison with different pitch angles is also performed.

2. Tunnel Model

The tunnel length and inclination are 1,280 m and -0.5%. For smooth numerical analysis, however, an actual tunnel inclination of 0% has been assumed. Also the jet fan adopted in this tunnel has a diameter of 1,030 mm, rated airflow of 36.8 m^3/s, pressure of 55 mmAq and 1,500 rpm. Fig. 1 shows the tunnel sketch. and Fig. 2 shows the computational domain in this study.

For representing the environmental air, the inlet is extended each direction as shown in Fig. 2. The section of the extended area is sufficiently large and the normal velocity through the inlet surface is to be small. The location of the jet fan is about 320 m from the entrance of the tunnel. For convenience sake, the total length of the tunnel is 1,200 m. The outlet of the tunnel is placed about 900 m downstream from the jet fan exit. The flow at the outlet is certainly uniform and thus, the extended outlet is unnecessary.

3. CFD Analysis

3.1 Governing Equations and Boundary Conditions

In this study, the three-dimensional computational fluid dynamics is employed. The flow in the tunnel ventilation is assumed to be steady, incompressible and turbulent. The related

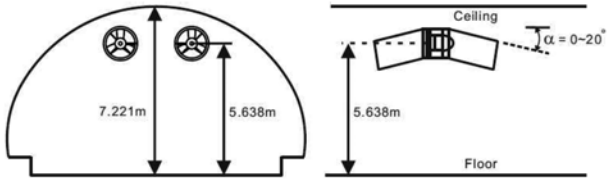

Fig. 1. Tunnel Sketch (Not to Scale)

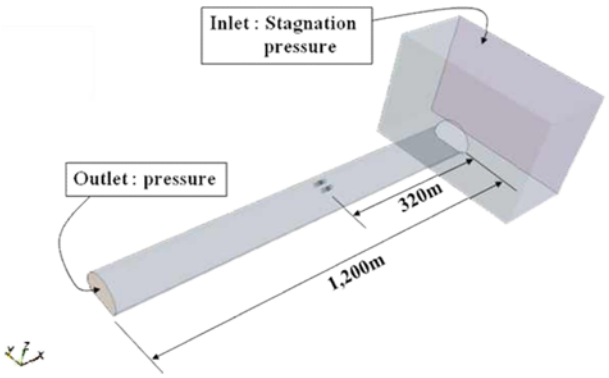

Fig. 2. Computational Domain

fluid properties are taken to be constant. The Reynolds-averaged continuity and momentum equations governing the three-dimensional turbulent flow can be written in Cartesian form as follows:

Continuity equation:

$$\frac{\partial}{\partial x_i}(\rho u_i) = 0 \tag{1}$$

Momentum equations:

$$\frac{\partial}{\partial x_i}(\rho u_j u_j) = -\frac{\partial p}{\partial x_i} + \frac{\partial \tau_{ij}}{\partial x_j} \tag{2}$$

where τ_{ij} is given by:

$$\tau_{ij} = -(\mu + \mu_t)\left(\frac{\partial u_i}{\partial x_j} + \frac{\partial u_j}{\partial x_i}\right) - \frac{2}{3}\rho k \delta_{ij} \tag{3}$$

In the above equations, u_i represents the time-averaged velocity components in the x, y and z directions, respectively; p and ρ are the pressure and the density of air flow. The turbulent viscosity coefficient, μ_t, is defined as:

$$\mu_t = C_\mu \rho \frac{k^2}{\varepsilon} \tag{4}$$

where k and ε represent the kinetic energy of turbulence and its dissipation rate, respectively. In order to obtain these quantities, the standard k-ε turbulent model (Launder and Spalding, 1974) is used.

For the flow analysis in the CFD calculation, and the used boundary conditions are shown in Table 1. Computational grid in this numerical calculation used about 1.2 million cells. To valid CFD models used in this study, the mesh dependency test with three different consequent numbers of cells (0.75 M, 1.2 M, and

Table 1. Input Boundary Conditions

Input items	Boundary conditions
Tunnel wall and floor	No-slip condition apply with function (smooth wall)
Air temperature inside tunnel	20 [℃]
Tunnel inlet/outlet	Atmospheric pressure boundary condition
Jet fan	Apply momentum source

Table 2. Mesh Dependency Test (α = 0)

Items	Coarse	Base	Refine
Mass flow rate [kg/s]	526.1	529.1	530.7
Friction (Ceiling) [N]	890.9	901.1	907
Number of Cells	759k	1200k	1700k

1.7 M) has been performed. The mass flow rate and friction on the ceiling are listed in Table 2. Results (mass flow rate and friction) are converged as increasing the number of cells. To save the computation time, 1.2 million cells are used here after. Flow in a tunnel is turbulent so that the Reynolds averaged Navier-Stokes equation should be calculated for a steady and low mach-number flow. In this study, the flow domain is divided into two regions such as near wall and fully turbulent regions and adopted a standard turbulent model and wall function.

3.2 Numerical Analysis Method

This research uses the STAR-CCM+ (Computational Dynamics Ltd., 2009), a commonly used CFD code, to solve the governing equation listed above. The moving grid method do not need any additional information for the computation except precise geometrical information such as 3D blade, jet fan duct shape, hub and so on, but it takes a huge amount of time to get stationary flow. On the other hand, using fan performance curve is required a precise fan performance curve from experiment previously. To save the computational resource, this research uses the method of the momentum source and the constant value of the momentum source (4000 kg/m^2s^2) is applied to the domain in the jet fan. This method cannot resolve the rotating effect, but can properly mimic the macroscopic flow in the tunnel such as pressure deviation, velocity profile at the downstream and so on. To compute the convective scheme of the governing equation, a second order upwind differencing scheme was used and to obtain the velocity field and pressure field, the SIMPLE algorithm (Patankar, 1980) was used. The convergence criterion for a computation was set to the condition when both the sum of fluid momentum at each cell normalized by momentum at the inlet and sum of fluid momentum in the continuity equation are 10^{-3} or below. Constant pressures are used for inlet boundary and outlet boundary. The fan, which is installed in the middle of the tunnel and is the only source of the air flow, sucks the air around it and the pressure goes down. Thus the air with high pressure at the inlet is entrained into the tunnel. The accuracy and efficiency of the computational results are also dependent on how the grid system is constructed. For the purposes of the accurate and

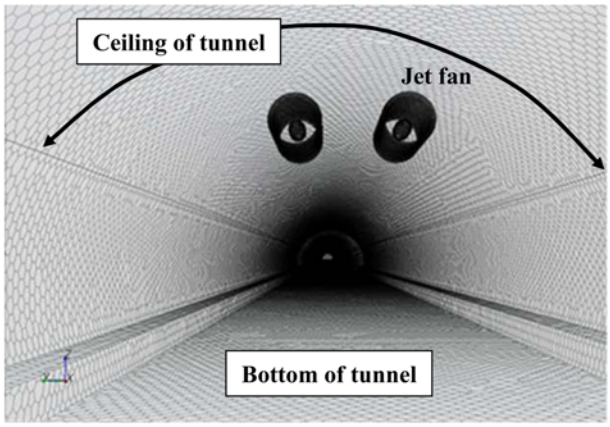

Fig. 3. Locally Refined Polyhedral Grid

effective computation, non-uniform grids (refined next to the tunnel wall and jet fan) are used as shown in Fig. 3. The number of grids is about 1.2 million and the 3 layers of the high-aspect ratio grid to represent the boundary layer properly are employed.

4. Results and Discussion

In the longitudinal ventilation system, a jet fan is an important instrument entraining fresh air from the atmosphere. The wall friction, recirculation from jet fan exit to entrance (Eck, 1973; Kweon *et al*., 2006), flow loss due to secondary flow, cars in the tunnel (Chen *et al*., 1998) show strong influence on the air entrainment. In this study, the computational analysis considering pitch angle variations of the inlet and outlet of the jet fan has been performed.

To examine the change of airflow in the tunnel dependent on the pitch angle (α) of a jet fan, the airflow inside the tunnel is indicated in Fig. 4. The pitch angles of the intake and exhaust of the jet fan is plotted in Fig. 1. Considering manufacturing processes in this study, both intake and exhaust angle are same and thus, one angle is sufficient to describe the pitch angle. The outlet of the jet fan has a high dynamic pressure of the jet fan, and as it moves downstream gradually loses velocity due to the wide section area and wall friction and thus, dynamic pressure changes to static pressure. Generally the pressure inside the tunnel shows a sudden drop after the air passes through the jet fan, which has the effect of entraining the external air (Ryu *et al*., 2003). Therefore, when the energy loss from the air flowing out from the jet fan is low, more air can be pulled into the tunnel.

As shown in Fig. 4, when the pitch angle of the jet fan is zero degrees, the mass flow rate is relatively low because the discharged airflow interacts strongly with the tunnel next to jet fan, and the interaction prevents airflow from forming the pressure to entrain a sufficient amount of fresh air. Therefore, the airflow in the jet fan increases but the airflow inside the tunnel decreases. On the other hand, when the pitch angle is high, interactions between discharged air and tunnel bottom is strong instead of a ceiling, and it prevents the pressure deviation to entrain air through the tunnel. On the other hand, the recircula-

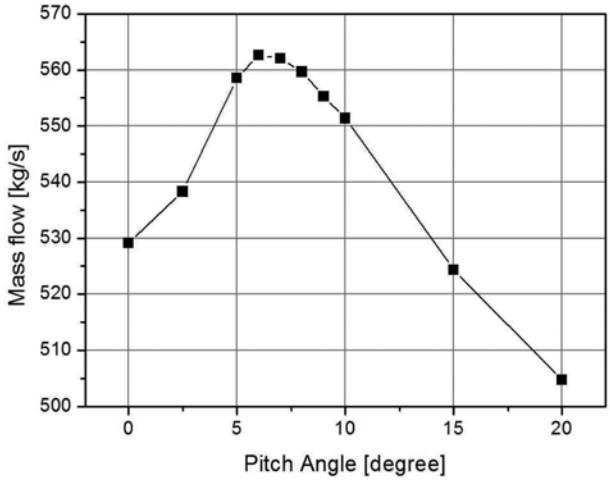

Fig. 4. Mass Flow Rate of Tunnel by Fan Pitch Angles

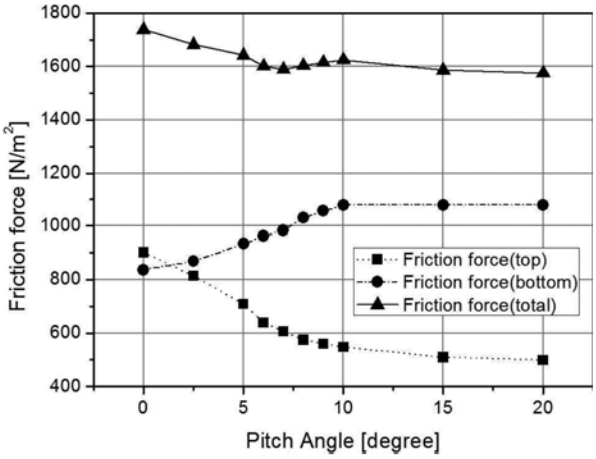

Fig. 5. Friction Force on the Walls by Fan Pitch Angles

tion from jet fan exit to inlet is critical for the jet fan performance (Kweon *et al.*, 2006; Byun *et al.*, 2007). However, in this study, the re-circulation is not observed. The high airflow entrainment is obtained at 6° where the airflow rate through the jet fan is relatively low but the interaction and wall friction with the tunnel wall is low.

Figure 5 shows the tunnel friction according to the pitch angle. The wall areas are divided top (ceiling) and bottom for calculating wall friction as shown in Fig. 3. Basically, the wall can be divided three parts such as top (crown of the tunnel), side and bottom (road) but the friction effect of the side wall is not significant. Therefore, two parts are considered in this study: top and bottom (bottom includes the side wall). As the pitch angle increases, the total friction loss decreases gradually and the lowest is at $\alpha = 6°$. The friction on the ceiling decreases, but the friction on the bottom increases until $\alpha = 10°$. These changes in friction force are closely related to the airflow discharged from the jet fan and the velocity near the tunnel wall. When the pitch angle is low, the high velocity air out of the jet fan directly meets the tunnel wall and it shows the highest loss from friction.

The pressure distributions along the tunnel are plotted in

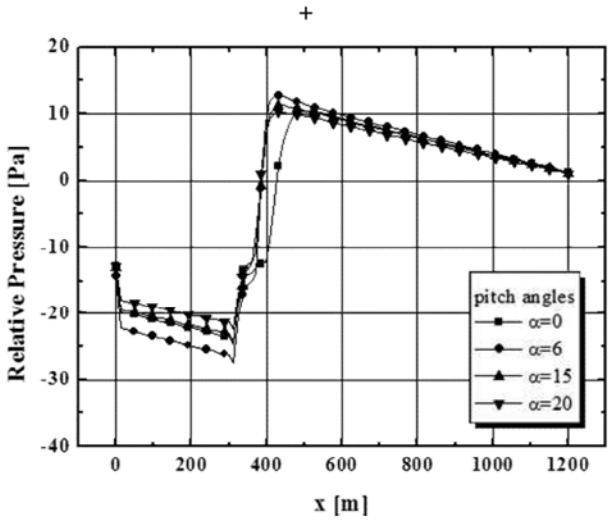

Fig. 6. Pressure Distribution along the Tunnel

Fig. 6. The 10 cases of the computational calculation with the different pitch angles are performed from $\alpha = 0°$ to 20°. To reduce the complexity by multiple lines in Fig. 6, only a few significant results (0°, 6°, 15° and 20°) are shown in Fig. 6. The jet fan is placed 320 m downstream from a tunnel entrance and thus, the static pressure suddenly increases after the jet fan as shown in Fig. 6. The pressure goes down linearly from the entrance until the jet fan and the low and negative pressure is the key factor of entraining the fresh air next to the entrance. The air passing through the jet fan gets momentum and increases the velocity. The exhaust air from the jet fan and fresh air are mixed and exchange momentums each other. The average velocity of the air becomes slow and the pressure increases gradually along the tunnel. The negative pressure changes to positive pressure at 60 m from the jet fan (380 m from entrance) and the peak pressure is placed at 50 m downstream (430 m from entrance). These tendencies can be observed from all the cases except the pitch angle is zero which has a lot of flow interaction with the ceiling.

Next to the entrance, the considerable pressure variations from sudden sectional area changes can be observed. When the pitch angle is six which shows the largest amount of air entrainment, pressure is the largest negative value which has sufficient driving force pulling the fresh air. The cases of $\alpha = 0°$ and 15° show relatively large friction on ceiling and interaction on the bottom, respectively. Therefore, the air entrainment of $\alpha = 0°$ and 15° are relatively small. For $\alpha = 6°$, the outlet of a jet fan aims the center of tunnel in downstream and thus, the wall friction between air and wall can be minimized as well as the sufficient space for the inlet can be obtained. When the pitch angle is 20°, the air is easily coming into the inlet but the exhaust hits the bottom surface and the energy loss increases significantly. Interestingly, the exhaust air of $\alpha = 0°$ flows along the ceiling surface by Coanda effect and the air will not detach from the ceiling for a long time and thus, do not mix well with fresh air. The pressure rise is behind the others as shown in Fig. 6. The pressure rises by the jet fan

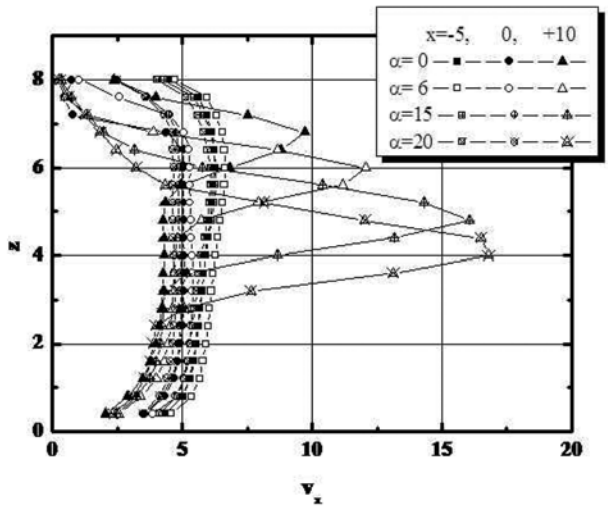

Fig. 7. Velocity Profiles according to Fan Pitch Angles

according to the pitch angles of 0°, 6°, 15°, and 20° are 17.3, 18.3, 16.9, and 15.6 Pa, respectively.

The velocity profiles at x = –5 (upstream), x = 0, and x = +10 (downstream) from the jet fan are plotted in Fig. 7 along the center of the tunnel. The pressure at x = +10 suddenly increases as shown in Fig. 6 and there are a large velocity peak by the exhaust. In case of $\alpha = 0°$, the peak is placed at the most top among them, but the peak value is small. On the contrary, in case of 20°, the velocity peak is placed at the center and the value is the largest. It is note that the velocity next to the ceiling of the jet fan becomes unusually low at $\alpha = 0°$, and 6°. Because there is no sufficient space for the air flow between two jet fans, both the pressure and the velocity are relatively low in this area. The air flow locally moves backward in the limited area instead of recirculation between exit and inlet of the jet fan.

The two significant factors for the energy loss in the tunnel are friction on the ceiling and an impact of exhaust air from the jet fan to the bottom. To reduce the energy loss, both friction and impact should be reduced. According to the pitch angle, both effects are varied and thus, mass flow rates (velocity profile) are changed. The velocity profiles in Fig. 7 are rearranged along the tunnel as shown in Fig. 8. When the pitch angle is 0°, the mixing between fresh and exhaust airs are slow because of the Coanda effect along the ceiling surface and did not finish until 430 m from entrance. Interestingly, there are negative velocity when the pitch angles are large ($\alpha = 15°$ and 20°). Since the exhaust air is strong and downward, there is a secondary flow between jet-like exhaust and ceiling. Therefore, the reverse flow reduces the effective sectional area for air flow and increases the energy loss. As the pitch angle increases, the contacting point between exhaust air from the jet fan and top of the tunnel is getting further. Therefore, the loss from friction is also suddenly reduced. When $5° < \alpha < 10°$, most of the airflow does not meet with the wall surface and flows downstream. However, the pitch

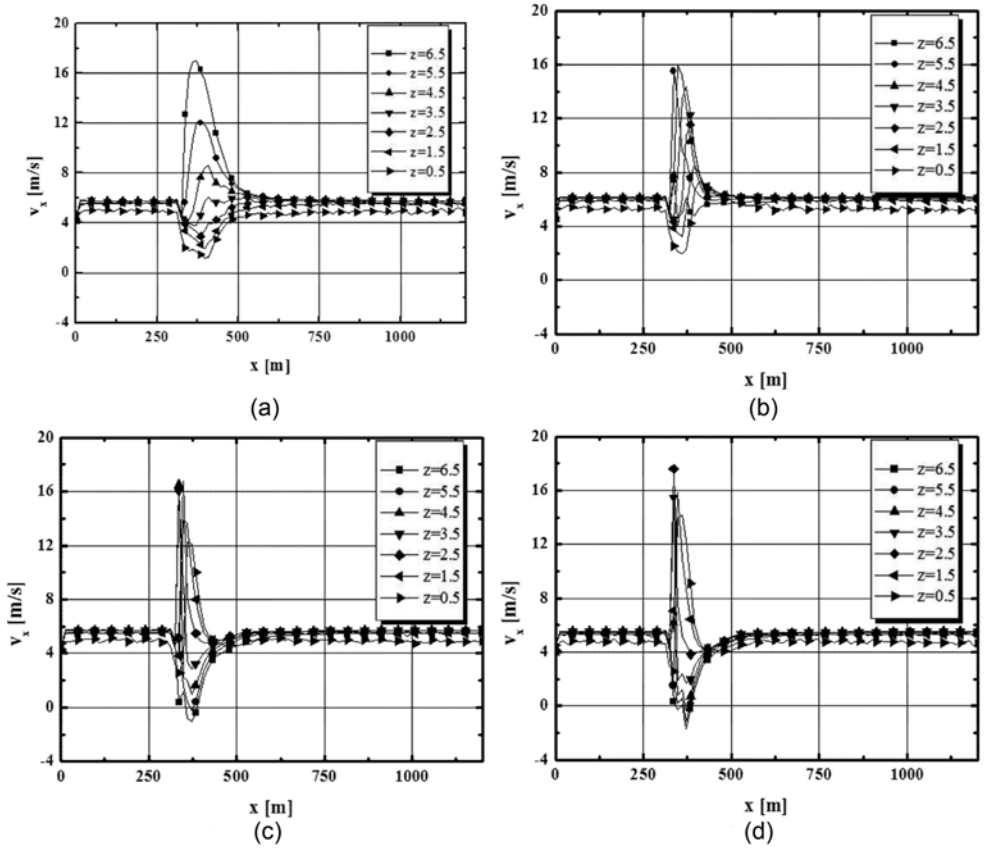

Fig. 8. Velocities along the Tunnel: (a) $\alpha = 0°$, (b) $\alpha = 6°$, (c) $\alpha = 15°$, (d) $\alpha = 20°$

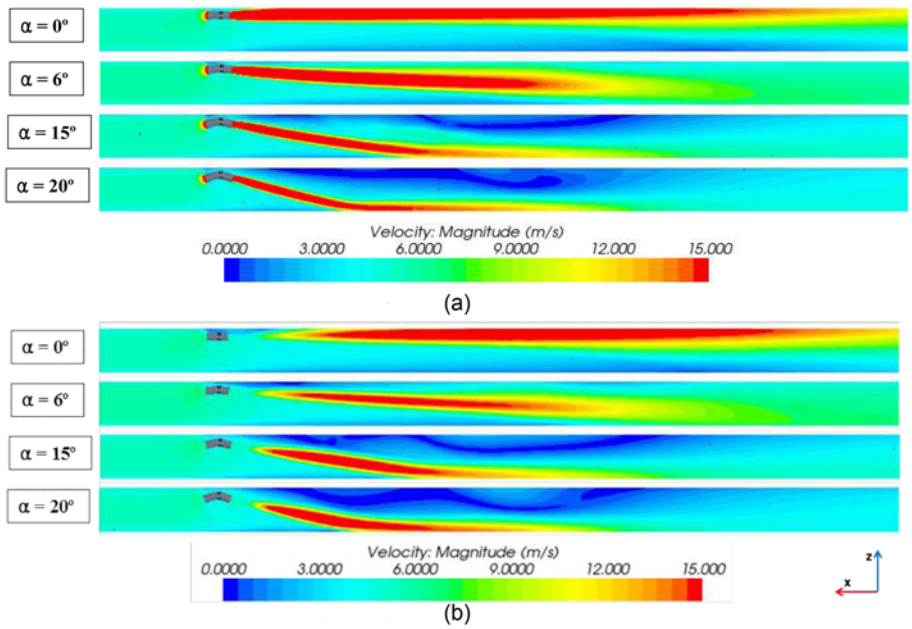

Fig. 9. Flow Field according to Pitch Angles of Jet Fan: (a) Velocity Contours at Center of Jet Fan, (b) Velocity Contours at Center of Tunnel

angle is excessively high ($\alpha \geq 15°$), the airflow meets the bottom surface instead of the ceiling. In this case, the high velocity air discharged from the jet fan has already been converted to static pressure from dynamic pressure due to the wide section area of the tunnel, significantly reducing the loss from friction compared to the case of $\alpha = 0°$. Therefore, the friction loss in Fig. 5 is obtained.

To visualize the friction loss of the tunnel wall and the recirculation of the fan entrance, the velocity of the tunnel section area is shown in Fig. 9. Fig. 9 (a) shows the airflow at the section where the fan is installed. When $\alpha = 0°$, the air flowing from the fan meets the ceiling directly but when $\alpha = 20°$, the air meets the bottom part of the tunnel. When $\alpha = 6°$, the air does not directly meet the bottom nor the ceiling, and shows a relatively smaller loss from friction. What is unique is that when $\alpha = 0°$, the air flowing from the fan does not meet any specific point and follows the ceiling for a long distance. This is thought to be from the Coanda effect between the wall and the fluid. Therefore, relatively more wall loss exists. Also, there is a surface with relatively low velocity at the bottom of the tunnel. When $\alpha = 20°$, the airflow meets not the ceiling but the bottom of the tunnel.

Figure 9 (b) shows the velocity distribution at the center of the tunnel. It shows a similar tendency as the velocity at the center of the fan, but with lower values. The downstream velocity of the top and bottom become similar first when $\alpha = 6°$ where the airflow is the highest. On the other hand, when $\alpha = 0°$ where the air meets the top of the tunnel and when $\alpha = 20°$ where it meets the bottom of the tunnel, the airflow is still not consistent with a deviation between top and bottom even as it moves significantly downstream.

As seen in Fig. 10, the negative pressure generated from the upstream of the jet fan plays a key role in the entrainment of external air into the tunnel as mentioned above. Depending on the pitch angle, the pressure at the top and bottom of the jet fan shows the lowest (–) pressure value at $\alpha = 6°$ at the top. And the pressure significantly increases (suction force reduces) at other angles at the top. This is mainly because the energy of the jet fan is not efficiently used as described above and is reduced from the loss by friction and recirculation. The location where the pressure changes from (–) to (+) downstream becomes shorter as the pitch angle increases. Especially when $\alpha = 20°$, the pressure recovers quickest to (+) as it hits the bottom of the tunnel, but due to loss, the pressure cannot reach a sufficiently high pressure. A similar trend is shown at the center of the tunnel. Also, the pressure difference between the upstream and downstream of the jet fan is relatively less compared to other cases. This is because the airflow from the bottom with a high dynamic pressure overcomes the pressure difference to rise up to the top, easily resulting in recirculation.

5. Conclusions

This study analyzed the effects of air inflow to the tunnel depending on the pitch angles of a jet fan by using the computational methods. Pressure decreasing along the tunnel from entrance to jet fan is entraining fresh air in to the tunnel. Friction loss on the wall surface, energy loss by jet-like flow hitting the bottom surface, and the reverse flow next to the inlet of the jet fan are decreasing the rate of pressure drop. According to the pitch angles, the pressure and the mass flow are varied. On the other hand, pressure recovery by dynamic pressure to static pressure at the downstream is altered with respect to the energy loss and Coanda effect. The discharged air from a jet fan was the highest at $\alpha = 0°$ where the loss from the jet fan itself was the

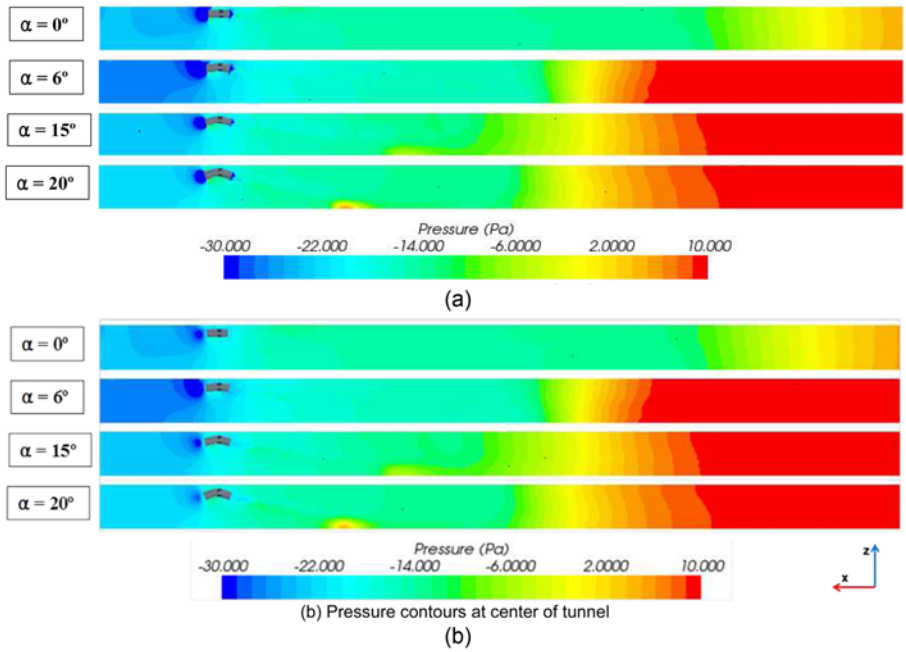

Fig. 10. Pressure Distribution according to Pitch Angles of Jet Fan: (a) Pressure Contours at Center of Jet Fan, (b) Pressure Contours At Center of Tunnel

lowest. But the airflow of the tunnel was the highest at $\alpha = 6$. This is due to the significant energy loss from friction at the top of the tunnel when the pitch angle of the jet fan is low ($\alpha = 0°$) and significant energy loss from dynamic pressure hiting the bottom surface directly, rather than friction loss, when the pitch angle is high ($\alpha = 20°$). Therefore, the highest level of airflow is at $\alpha = 6°$ where the loss from both is the least. On the other hand, the Coanda effect, which attaches the air flow on the ceiling considerablely long distance of downstream increases the firction and prevents the entrainment of the fresh air.

In this study, considering only the jet fan and the tunnel itself, the optimal angle will be varied as including vehicles or other obstacles in the tunnel. The studies considering the blockage effect by the vehicles which are source of the polluted air are required in the near future.

Acknowledgements

This research was supported by a grant from the 2014 academic program in Kangwon National University.

References

Byun, J. S., Lim, H. J., Kang, S. H. and Lee, J. H. (2007). "Analysis of smoke control according to jet fan location in straight long tunnel." *Korean Journal of Air-Conditioning and Refrigeration Engineering*, Vol. 19, No. 9, pp. 662-668.

Chen, T. Y., Lee, Y. T., Hsu, C. C. (1998). "Investigations of piston-effect and jet fan-effect in model vehicle tunnels." *Journal of Wind Engineering and Industrial Aerodynamics*, Vol. 73, pp. 99-110.

Computational Dynamics Ltd. (2009). *STAR-CCM+ Version 4.02 user manual*, Computational Dynamics Ltd.

Eck, B. (1973). *Fans*, Pergamon Press, New York, N.Y.

Kweon, O. S., Yoon, C. H., Yoon, S. W., and Kim, J. (2006). "Model test for the determination of distances between jet-fans and analysis of recirculation." *Tunnelling Technology*, Vol. 8, No. 4, pp. 335-344.

Launder, B. E. and Spalding, D. B. (1974). "The numerical computation of turbulent flows." *Computer Methods in Applied Mechanics and Engineering*, Vol. 3, pp. 269-289.

Patankar, S. V. (1980). *Numerical heat transfer and fluid flow*, McGraw Hill, New York, N.Y.

Ryu, J. H., Yoo Y. H., and Kim, J. (2003). "The jet-fan model test for a tunnel ventilation." *Korean Journal of Air-Conditioning and Refrigeration Engineering*, Vol. 15, No. 8, pp. 630-640.

Se, C. M. K., Lee, E. W. M., Lai, A. C. K. (2012). "Impact of location of jet fan on airflow structure in tunnel fire." *Tunnelling and Underground Space Technology*, Vol. 27, pp. 30-40.

Wang, F., Wang, M., He, S., Zhang J., and Deng, Y. (2010). "Computational study of effects of jet fans on the ventilation of a highway curved tunnel." *Tunnelling and Underground Space Technology*, Vol. 25, pp. 382-390.

Witt, K. C. and Schutze, J. (2006). "Bend it like a banana." *12th International Symposium on Aerodynamics and Ventilation of Vehicle Tunnels*, Portoroz, Slovenia, pp. 683-693.